Sensors and Actuators A 181 (2012) 1–5

Contents lists available at SciVerse ScienceDirect

Sensors and Actuators A: Physical

journal homepage: www.elsevier.com/locate/sna

Interaction between gas flow and a Lamb waves based microsensor

Lianqun Zhou[a,b,c,1], Jean-François Manceau[c,*], François Bastien[c]

[a] Changchun Institute of Optics, Fine Mechanics and Physics, Chinese Academy of Sciences, Changchun 130033, China
[b] Graduate University of Chinese Academy of Sciences, Beijing 100039, China
[c] MN2S Department, FEMTO-ST Institute, CNRS, Université de Franche-Comté, ENSMM, UTBM – 32 Avenue de l'Observatoire, 25044 Besançon, France

ARTICLE INFO

Article history:
Received 1 September 2011
Received in revised form 11 April 2012
Accepted 13 April 2012
Available online 20 April 2012

Keywords:
Surface acoustic wave
Lamb wave
Microsensor
Gas flow

ABSTRACT

The interaction between the gas flow and Lamb waves is investigated in this paper. Depending on the fact that the phase velocity is higher or lower than the gas sound velocity, we will get evanescent waves (EW) or leaky Lamb waves (LLW) in the gas along the solid–gas interface. In the LLW case, experiments showed that gas flow had not evident effects on Lamb waves' propagations. In the EW case, the interaction between the gas flow and the Lamb waves was observed clearly when the Lamb wave phase velocity is close to the gas sound velocity. This interaction is related with the gas flow velocity profile within the boundary layer. The experimental results show that this sensor is very promising for many experiments involving gas flows such in wind tunnels, micro channels characterization, and can lead to multi-parameters measurements.

1. Introduction

Aerodynamics has a long history from macroscopic to microscopic scale, especially in gases vortex flows, wind tunnel experiments or flows within microchannels [1–4]. In macroscopic aerodynamics fields, hot wire anemometry or calorimetric sensor are mainly adopted [5–8], and the measurement of the sensor's temperature is used to give the flow. For this kind of sensor, it is difficult to distinguish the temperature and fluid velocity vector effects. In microscopic flow, micro-fluidic devices are becoming increasingly common and are seen in applications ranging from biology to nanotechnology and manufacturing [4,9]. Micro-particle image velocimetry is one well-established technique to investigate the fluid flow, but this method needs special flow-tracing particles [9–12]. Surface acoustic waves (SAW) or flexural wave gas flow meter use the temperature effect of gas cooling due to flow [13–15]. The gas detection itself is not direct but use detection layer for example a palladium silver alloy layer for hydrogen [16]. The use of sound for measurement of flow in the boundary layer has been proposed by some authors [17,18] but in this paper we use an evanescent wave generated with a Lamb wave that gives the opportunity to change the penetration depth. Lamb waves have been used for fluid parameters measurements [19] and our previous work suggested that the gases layers could have apparent effects on Lamb waves' propagations [20]. At present, there are no reports about the gas flow effects on the Lamb waves' propagation. In this paper, we study the effect of flowing along a membrane supporting Lamb wave propagation.

When Lamb waves propagate in a membrane with a wavelength much greater than the thickness of the membrane (d), two basic propagation modes exist in the membrane, the antisymmetric mode (A_0) and the symmetric mode (S_0). In S_0 mode, the effect of static gas layers on the Lamb waves' propagation does not change the phase velocity [21]. When the Lamb wave phase velocity (c_{LW}) of the antisymmetric mode (A_0) is less than the gas sound velocity (c_f) an evanescent acoustical wave (EW) exists in the gas near the solid–gas interface. The evanescent wave intensity exhibits exponential decay with distance from the boundary where the wave is formed and propagates in the same direction and at the same speed with the Lamb wave. As the EW propagates along the gas–solid interface, it can provide an attractive tool for gas dynamics research. When the frequency is high enough and c_{LW} becomes higher than c_f, the waves can be considered as a leaky Lamb waves (LLW). Its behavior with the flow is also an interesting question to be investigated. Some experiments for this range of operation will be discussed in this paper. Let us define the boundary layer thickness and the acoustic evanescent penetration depth before theoretical analysis.

2. Principle

2.1. Boundary layer thickness of a gas flow

Let us consider Lamb wave sensor placed in a gas that flows along a flat surface aligned with the flow direction (x direction), see

* Corresponding author. Tel.: +33 381853955.
E-mail address: jfmanceau@femto-st.fr (J.-F. Manceau).
[1] Present address: Suzhou Institute of Biomedical Engineering and Technology, Chinese Academy of Sciences, Suzhou 215000, China.

0924-4247/$ – see front matter © 2012 Elsevier B.V. All rights reserved.
http://dx.doi.org/10.1016/j.sna.2012.04.013

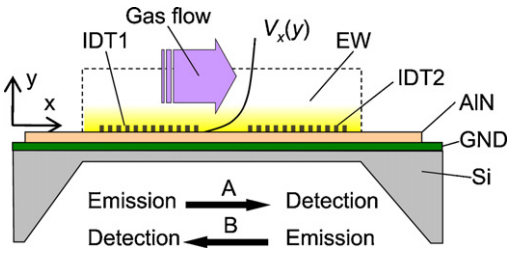

Fig. 1. The Lamb wave based sensor with the gas flow boundary layer, experimental membrane thickness (IDT: 0.2 μm, AlN: 1.8 μm, GND: 0.2 μm, Si membrane: 12 ± 3 μm) and IDT period: 400 μm.

Fig. 1. Under the assumption of no slip at the gas–solid interface, the velocity gradients appear near the surface in y direction, see Fig. 2. We assume that this gradient remains constant along the length L of the membrane.

The flow can be conceptually divided into two parts which is separated by an imaginary surface (the dashed line in Fig. 2). The first part is the free stream zone, in which the gas velocity is constant (V_0). The second part is the boundary layer, in which the velocity ($V_x(y)$) varies from zero at the wall to a velocity equal to that of the free stream. The flow is supposed to be laminar flow within the boundary layer thickness h_{BL} and the profile of the boundary layer supposed to be constant along the length of the sensing area. The velocity function $V_x(y)$ in the boundary layer is assumed to be as [22]:

$$V_x(y) = V_0 \sin\left(\frac{\pi y}{2h_{BL}}\right) \quad \text{with } 0 \le y \le h_{BL} \tag{1}$$

2.2. Acoustic evanescent wave penetration depth for Lamb wave

When the acoustic wave propagates in static fluid, the displacement at the surface ($y = 0$) can be expressed as the following formula:

$$u(x, y, t) = U_0 \exp(i(k_x x + k_y y - \omega t)) \tag{4}$$

In which, U_0 is an arbitrary amplitude, k_x and k_y wave number in x and y direction, The relation between wave numbers must verify $k_f^2 = k_x^2 + k_y^2$ where $k_f = \omega/c_f$ is the wave number for the waves propagating within the fluid (gas or liquid). In our case, $k_x = k_{LW} = \omega/c_{LW}$, the wavenumber and c_{LW} the phase velocity for the Lamb wave propagation. Let us consider an interesting generalization of Eq. (4) for the case when $c_{LW} < c_f$ ($k_{LW} > k_f$). The wavenumber $k_y = \sqrt{k_f^2 - k_{LW}^2} = i\sqrt{k_{LW}^2 - k_f^2}$ is then purely imaginary and the acoustic wave is

$$u(x, y, t) = U_0 \exp(-|k_y| y) \exp(i(k_{LW} x - \omega t)) \tag{5}$$

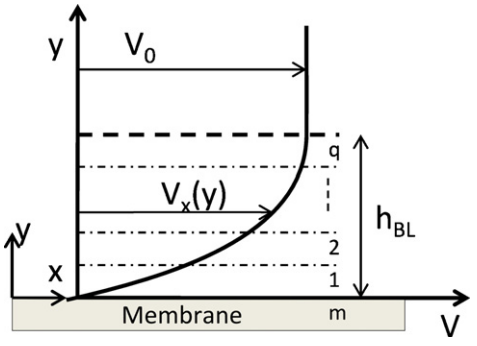

Fig. 2. Flow boundary layer above a thin membrane at a given position in wind direction, the wind velocity changes with the distance (y) from the plate surface.

The amplitude decrease exponentially with the distance from the surface, this wave is called evanescent wave (EW). The term $\delta_E = 1/k_y$ is called evanescent wave penetration depth and can be expressed as

$$\delta_E = 1/k_y = \frac{\lambda_{LW}}{2\pi} \frac{1}{\sqrt{1 - (c_{LW}/c_f)^2}} \tag{6}$$

With λ_{LW} the length wave of the Lamb wave. When the gas flows over the Lamb wave sensor, the gas flow will interact with the evanescent wave. The ratio between the flow velocity boundary layer thickness h_{BL} and the evanescent wave penetration depth (δ_E) is an important factor affecting this interaction. It is important to underline that our theory gives a good explanation of the behavior of Lamb wave with a gas flow but the precise value of frequency shift in the region where c_{LW} is close to c_f is not obtained for several reasons. (i) The theory assume a wave coming from infinity. This assumption is a good approximation for rapidly decreasing evanescent wave but become poor when the evanescent wave extends as c_{LW} is close to c_f and (ii) the standing wave ratio is not well defined because the reflection of the evanescent wave in the gas at the end of membrane is not clearly established.

2.3. Calculations for Lamb wave interaction with gas flow

In this paper, we try to survey the gas flow interaction with device described in Fig. 1. The device contains a silicon membrane with a ground layer (Ti/Mo) and a piezoelectric layer (aluminum nitride, AlN). Lamb waves are excited and detected directly using inter-digital transducers (IDTs) [23,24].

As waves are partly reflected at the end of length-limited membrane, the response includes traveling waves and standing waves. When the Lamb waves propagate in a membrane with gas flow on the top surface, the evanescent wave (EW) distribution could be modified by the gas flow. Based on the following assumptions, this physical problem can be analyzed theoretically at least as a first approximation. The equations of motion for each material are written in terms of scalar potential function φ and vector potential function ψ [21,25,26]. Usually the potential functions are introduced for isotropic materials. This assumption is possible here because the Lamb wave travels in the membrane only along one direction in which the energy propagate in the direction of wave number vector.

The particle displacement vector $\mathbf{u}$ for the membrane and fluid are as functions of potentials written in form

$$\begin{aligned} \boldsymbol{u}_m &= \text{grad}\varphi_m + \text{curl}\psi_m \\ \boldsymbol{u}_f &= \text{grad}\varphi_f \end{aligned} \tag{7}$$

where the subscripts m and f, refer to the membrane and fluid respectively. As the wave is in one plane and the motion does not depend on the coordinate z, the component of the vector potential along the z-axis only will have a non-zero magnitude; we denote this component simply by ψ. The potentials φ and ψ are called the potentials of longitudinal and shear waves respectively, and satisfy the following wave equations:

In the membrane

$$\begin{aligned} \nabla^2\psi_m &= \frac{1}{c_t^2}\frac{\partial^2\psi_m}{\partial t^2} \\ \nabla^2\varphi_m &= \frac{1}{c_d^2}\frac{\partial^2\varphi_m}{\partial t^2} \end{aligned} \tag{8}$$

In the fluid

$$\nabla^2\varphi_f = \frac{1}{c_f^2}\frac{\partial^2\varphi_f}{\partial t^2} \tag{9}$$

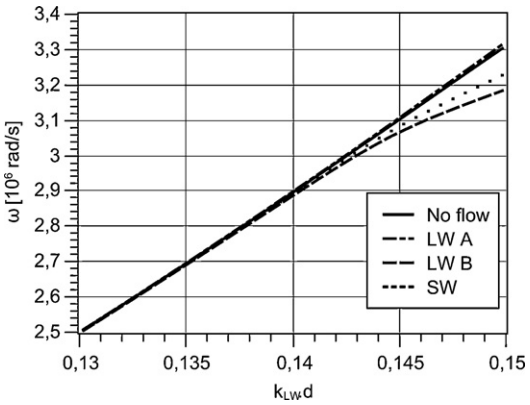

Fig. 3. Theoretical dispersion curves for different cases: when the there is no flow (solid), when the gas flow direction is the same as propagation direction (LWA) (dashed-dotted) or the reverse (LWB) (dashed), and finally for standing waves case (SW) (dotted).

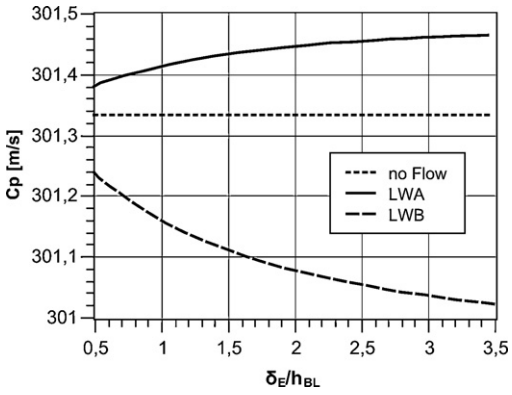

Fig. 4. The Lamb wave phase velocity changes with the ratio δ_E/h_{BL}, when $k_{LW}\cdot d = 0.135$ (k_{LW}: wave number, d: membrane thickness). The gas flow direction is the same as propagation direction (LWA) or the reverse (LWB).

where c_d and c_t are the velocities of longitudinal (dilatational) and transverse (shear) waves of the membrane, c_f is the fluid sound velocity.

When there is a flow with a boundary layer, the sound velocity varies continuously inside the fluid. At a first approximation, this continuity is replaced by several layers in which the sound velocity is treated as the average value of apparent sound velocity in that layer. The membrane and gas flow will be approximated as a membrane with q layers of fluid within the flow boundary layer thickness h_{BL}, see Fig. 2.

If $c_{LW} = \omega/k_{LW} < c_f < c_t < c_d$, the solutions to Eqs. (8) and (9) can be expressed as:

In the membrane,

$$\varphi_m = (Ae^{-\sqrt{k_{LW}^2-(\omega^2/c_d^2)}y} + Be^{\sqrt{k_{LW}^2-(\omega^2/c_d^2)}y})\cos(k_{LW}x-\omega t)$$
$$\psi_m = (Ce^{-\sqrt{k_{LW}^2-(\omega^2/c_t^2)}y} + De^{\sqrt{k_{LW}^2-(\omega^2/c_t^2)}y})\sin(k_{LW}x-\omega t) \quad (10)$$

And in the fluid, for each nth layer of fluid as

$$\varphi_{fn} = (A_{fn}e^{-\sqrt{k_{LW}^2-(\omega^2/c_f^2)}y} + B_{fn}e^{\sqrt{k_{LW}^2-(\omega^2/c_f^2)}y})\cos(k_{LW}x-\omega t) \quad (11)$$

These solutions should satisfy the boundaries conditions for the stresses τ and the displacements u at the interfaces. At the membrane (subscript m)-fluid (subscript f) interface, the conditions are, $\tau_{f1} = \tau_{myy}$, $\tau_{myx} = 0$ and $u_{f1y} = u_{my}$, between fluid layer 1 and fluid layer 2, boundaries conditions to be satisfied are $\tau_{f1} = \tau_{f2}$ and $u_{f1y} = u_{f2y}$, and similar conditions for each fluid–fluid interface.

Considering the boundary conditions to all interfaces, we will get a set of simultaneous homogeneous equations where A, B, C, D, A_{fn} and B_{fn} are unknowns. In our case, with one side of the membrane with n layers of fluid, we get $3+2n$ boundary conditions and $3+2n$ unknown parameters. This set of equation will have non-zero solution when the determinant associated with the equation system is zero. An implicit function between k_{LW} and ω is obtained, that is to say the dispersion equation.

We have computed the dispersion equation for travelling waves with a given flow in two configurations A and B as shown in Fig. 1. The gas flow velocity V_0 for calculation is 20 m/s. The sound velocity in still air is taken at 340 m/s. The angular frequency ω is plotted as a function of the product $k_{LW}\cdot d$ with d the membrane thickness (see Fig. 3). The effect is very different for the two cases depending on the flow either increase the apparent sound velocity or not.

Due to the limited length of the membrane, standing waves occurs. We use a simple model to investigate the influence of the gas flow on these standing waves. If there are resonances without the flow, the wavelength (λ) and the length of the membrane (L) should satisfy $\lambda = 2L/N$ and $f = c_{LW}\cdot N/2L$, where N is an integer corresponding to the rank of the mode.

With a gas flow, for the simple form of A_0 mode and perfect reflection, the displacement of the incident wave and the reflected wave along the x direction are supposed to be $A\sin(\omega t - k_1 x)$ and $-A\sin(\omega t + k_2\cdot x)$ respectively, where A is the amplitude, ω is the wave's angular frequency, t is time, k_1 and k_2 are wave number for the incident wave and the reflected wave. Accordingly the sum of the two waves is

$$A[\sin\omega t(\cos k_1 x - \cos k_2 x) - \cos\omega t(\sin k_1 x + \sin k_2 x)] \quad (12)$$

This equation can be rewritten as

$$-2A\sin\left(\frac{k_1+k_2}{2}x\right)\cdot\cos\left(\omega t - \frac{k_1-k_2}{2}x\right) \quad (13)$$

This equation should also satisfy the boundary conditions at both ends (borders) of the membrane where the displacement is zero at any time. For $x = 0$, this condition is always satisfied. When $x = L$, the k_1 and k_2 must have the following relationship

$$\frac{k_1+k_2}{2} = \frac{\pi n}{L} \quad (14)$$

The pseudo standing wave occurs when wave-number is $(k_1+k_2)/2$. With the known dispersion curves for the two directions for travelling waves, the solutions for standing waves is deduced easily by averaging the wave-numbers of the two directions for given angular frequency or velocity. As shown in Fig. 3, it indicates that the response of the system varies with the gas flow velocity even for pure standing waves.

The previous simple model shows that when the phase velocity of Lamb wave is below and close to sound speed in air, the Lamb wave is sensitive to the gas flow. The variation of the thickness of the boundary layer is introduced in the model. Obviously the effect of the flow decreases when the characteristic decaying length δ_E of the evanescent wave become small compared to the boundary layer thickness h_{BL} (see Fig. 4).

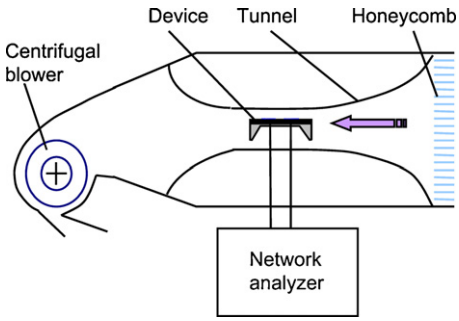

Fig. 5. Sketch of wind tunnel set-up for the wind flow experiments.

3. Experimental results and discussion

3.1. Wind tunnel set-up for gas flow measurements

An experimental set-up has been built to produce an air flow passing on the device's surface to study its effect (see Fig. 5). In order to change the relative direction between the main waves' propagation and the air flow, we choose to change the acoustic waves propagation direction by deciding which port of the IDT is the exciting port or the receiving port, as shown in Fig. 1, configuration *A* means IDT1 is emitter and IDT2 is receiver, configuration *B* means IDT2 is emitter and IDT1 is receiver. This method allows keeping the set-up in the same condition for the two directions. All experiments are performed at room temperature and at atmospheric pressure. Different frequencies responses of A_0 mode are used to check gas flow effects.

3.2. Measurements for different frequencies

The first experiment is done with a center frequency of 264 kHz where the wave velocity is near 240 m/s. It can produce the Evanescent Wave around the gas–solid interface. The experimental results demonstrate that the amplitude and phase responses are almost the same; no matter there is an air flow or not (see Fig. 6(a)).

Another measurement is performed at a higher frequency, 1.663 MHz that corresponds to a Lamb wave phase velocity greater than the sound velocity. The wave can be considered as a leaky Lamb wave, and the results show that there are still almost no changes for the different cases (see Fig. 6(b)). It is due to the fact that the leaky wave angle depends on the gas flow velocity at the surface of the membrane and this velocity is always zero in no slip condition.

A third experiment is done at a frequency of 510 kHz where the acoustic wave velocity is smaller but near the sound velocity of air (340 m/s). As indicated by simple theoretical calculations using Eq. (6), the EW depth δ_E in this region is larger than in the other cases [20]. The response at this frequency is shown in Fig. 6(c). The result demonstrates that the air flow has a remarkable influence on the amplitude and the phase response of the device.

3.3. Discussion

Although the waves are not purely traveling wave, our proposal is to measure the effect of the relative direction between the gas flow and the Lamb waves on frequency response. Note that the responses in the absence of air flow for these measurements are almost the same, when we invert the exciting and detecting IDT, see Fig. 6(a–c).

From the measurements, we show that the ratio δ_E/h_{BL} plays an important role in the response. The flow boundary layer thickness h_{BL} is a constant value as we keep the set-up in a fixed position

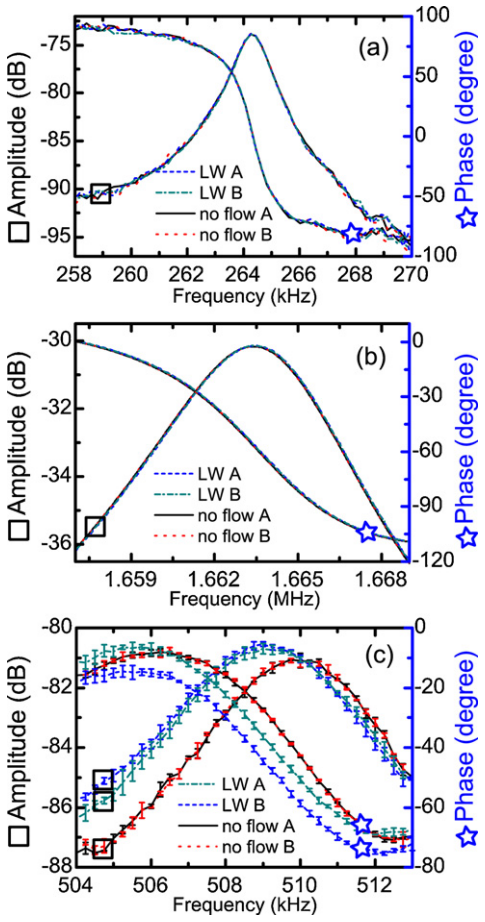

Fig. 6. Amplitude (with square) and phase (with star) measurements for different frequency ranges, (a) around 264 kHz, (b) 1.663 MHz and (c) 510 kHz, The gas flow direction is the same as propagation direction (LWA) or the reverse (LWB). Measurements are recorded without flow and with flow at a speed of about 20 m/s for each case.

and is estimated for a flow velocity of 20 m/s to be $h_{BL} = 410\,\mu m$ above the membrane. For the frequency of 264 kHz, c_{LW} is far away from c_f, but it is not the same when the frequency is 510 kHz, thus δ_E in the first case is smaller than in the second case. When δ_E/h_{BL} becomes higher, the Lamb wave propagation is more easily affected by the gas flow. This is in agreement with the prediction given by Figs. 3 and 4, even if the real case is more complex than our simple theoretical model. We have performed these experiments using another device, and the results confirm that the frequency shifts only when the phase velocity is near to the gas sound velocity.

In order to verify the repeatability of the measurement, we record the frequency corresponding to a given phase value as a function of time, as shown in Fig. 7(a). The result clearly shows that the response has good repeatability. Although the absolute responses for the two propagation directions change with time, we note that the difference (ΔF_{AB}) between the values of the frequency obtained consecutively for the two directions is more stable. The variation due to the room temperature is one of the main contributing factors to the changes of absolute frequency (about 95 ppm/°C) but its effect on the difference ΔF_{AB} stills neglectable.

The plot of the flow velocity versus ΔF_{AB} is shown in Fig. 7(b) up to a maximum velocity of about 20 m/s. The results show an almost linear relation between the flow velocity and the difference in the frequency measured for the two opposite directions. The measured sensitivity ($(\Delta F_{AB}/f_0)/\Delta V$) at the maximum flow velocity is about $80 \pm 7\ \text{ppm m}^{-1}\,\text{s}$, in which f_0 is the center frequency and ΔV is the

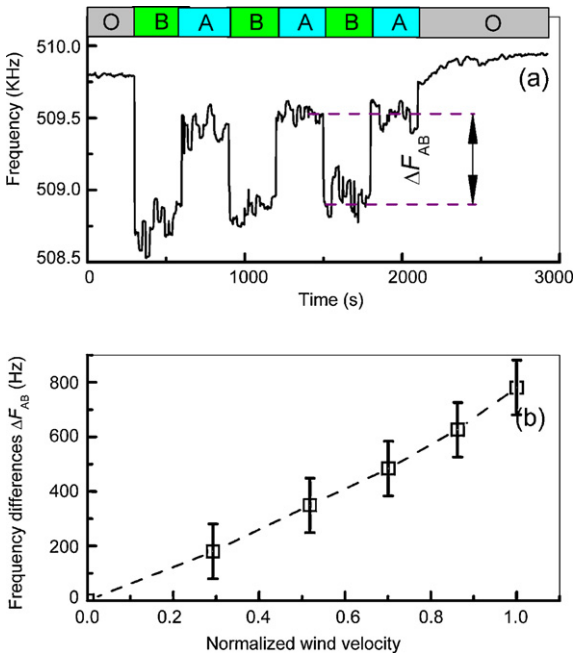

Fig. 7. The frequency changes at a given phase of −30° around the frequency of 510 kHz: (a) when the wind speed is about 20 m/s, the measured frequency shifts with time, A and B as shown in Fig. 1, O: no wind; (b) frequency difference between two consecutive excitation directions change with respect to the normalized wind speeds V/V_{max} (the maximum wind speed V_{max} is about 20 m/s).

velocity. This result shows that it is possible to use this device for precise and accurate aerodynamics measurements.

4. Conclusions

We reported the observed effects of gas flow on Lamb waves' propagation within a microsensor. This sensor is not based upon thermal effects but mainly on the interaction of the flow with an evanescent wave. For the evanescent wave case, the Lamb waves have a high sensitivity to the gas flow in the case where their phase velocities are close to the gas sound velocity. The ratio between the evanescent wave depth δ_E and the flow boundary layer thickness is an important factor affecting the sensitivity. The different EW depths obtained at different frequencies provide a powerful tool to investigate the properties of the flow boundary layers. Our work suggests that the Lamb waves based sensors could be used in aerodynamics, especially for wind tunnel, micro/nano channels and for multi-parameters measurements.

Acknowledgements

The authors gratefully acknowledge technical supports from Engineer Jean-Yves Rauch, Pascal Blind, Jean-Claude Baudouy and Professor Franck Chollet for valuable discussion. The authors also wish to thank the French Embassy PhD Program.

References

[1] M. Eckert, Theory from wind tunnels: empirical roots of twentieth century fluid dynamics, Centaurus 50 (2008) 233–253.
[2] J.H.B. Smith, Vortex flows in aerodynamics, Annual Review of Fluid Mechanics 18 (1986) 221–242, http://dx.doi.org/10.1146/annurev.fl.18.010186.001253.
[3] J.M. Wallace, P.V. Vukoslavčević, Measurement of the velocity gradient tensor in turbulent flows, Annual Review of Fluid Mechanics 42 (2010) 157–181, http://dx.doi.org/10.1146/annurev-fluid-121108-145445.
[4] Z. Zhang, H. Zhang, H. Ye, Pressure-driven flow in parallel-plate nanochannels, Applied Physics Letters 95 (2009) 154101.
[5] G. Comte-Bellot, Hot-wire anemometry, Annual Review of Fluid Mechanics 8 (1976) 209–231, http://dx.doi.org/10.1146/annurev.fl.08.010176.001233.
[6] S.A. Dixit, O.N. Ramesh, Large-scale structures in turbulent and reverse-transitional sink flow boundary layers, Journal of Fluid Mechanics 649 (2010) 233–273, http://dx.doi.org/10.1017/s0022112009993430.
[7] S. Gerashchenko, N.S. Sharp, S. Neuscamman, Z. Warhaft, Lagrangian measurements of inertial particle accelerations in a turbulent boundary layer, Journal of Fluid Mechanics 617 (2008) 255–281, http://dx.doi.org/10.1017/s0022112008004187.
[8] Y.-H. Wang, C.-P. Chen, C.-M. Chang, et al., MEMS-based gas flow sensors, Microfluidics and Nanofluidics 6 (2009) 333–346.
[9] S.T. Wereley, C.D. Meinhart, Recent advances in micro-particle image velocimetry, Annual Review of Fluid Mechanics 42 (2010) 557–576, http://dx.doi.org/10.1146/annurev-fluid-121108-145427.
[10] J.K. Arthur, D.W. Ruth, M.F. Tachie, PIV measurements of flow through a model porous medium with varying boundary conditions, Journal of Fluid Mechanics 629 (2009) 343–374, http://dx.doi.org/10.1017/s0022112009006405.
[11] O. Kimmoun, H. Branger, A particle image velocimetry investigation on laboratory surf-zone breaking waves over a sloping beach, Journal of Fluid Mechanics 588 (2007) 353–397, http://dx.doi.org/10.1017/s0022112007007641.
[12] R. Lindken, M. Rossi, J. Gro Westerweel, Micro-particle image velocimetry ([small micro]PIV): recent developments, applications, and guidelines, Lab on a Chip 9 (2009) 2551–2567.
[13] N.T. Nguyen, A.H. Meng, J. Black, R.M. White, Integrated flow sensor for in situ measurement and control of acoustic streaming in flexural plate wave micropumps, Sensors and Actuators 79 (2000) 115–121.
[14] J.G. Brace, T.S. Sanfelippo, S.G. Joschi, Surface acoustic-wave device for measuring of gas flow, Review of Scientific Instruments 62 (1991) 208–213.
[15] S.G. Joshi, Surface-acoustic-wave (SAW) flow sensor, IEEE Transactions on Ultrasonics, Ferroelectics and Frequency Control 38 (1991) 148–154.
[16] N. Yamamoto, Y. Nakagawa, S. Kakio, Hydrogen gas sensor using good characteristics of Lamb wave, Japanese Journal of Applied Physics 47 (2008) 4024.
[17] M.G. Smith, S. Whale, Acoustic measurement of boundary layer flow parameters, Journal of Sound and Vibration 301 (2007) 278–296.
[18] P.P. Geoghegan, W.J. Crowther, N. Wood, Measurement of boundary layer velocity profiles by ultrasonic tomography for the prediction of flow separation, in: 25th AIAA Aerodynamic Measurement Technology and Ground Testing Conference, San Francisco, California, June 5–8, 2006, pp. 1–14.
[19] T. Laurent, F.O. Bastien, J.-C. Pommier, A. Cachard, D. Remiens, E. Cattan, Lamb wave and plate mode in ZnO/silicon and AlN/silicon membrane: application to sensors able to operate in contact with liquid, Sensors and Actuators A: Physical 87 (2000) 26–37.
[20] L. Zhou, J.-F. Manceau, F. Bastien, Influence of gases on Lamb waves propagations in resonator, Applied Physics Letters 95 (2009) 223503–223505.
[21] M.F.M. Osborne, S.D. Hart, Transmission, reflection, and guiding of an exponential pulse by a steel plate in water. I. Theory, The Journal of the Acoustical Society of America 17 (1945) 1–18.
[22] L. Brekhovskikh, V. Goncharov, Mechanics of Continua and Wave Dynamics, Springer-Verlag, Berlin, 1985.
[23] K. Toda, Frequency characteristics of an interdigital transducer for Lamb wave excitation, Journal of Applied Physics 45 (1974) 5136–5140.
[24] R.M. White, F.W. Voltmer, Direct piezoelectric coupling to surface elastic waves, Applied Physics Letters 7 (1965) 314–316.
[25] P. Lloyd, M. Redwood, Wave propagation in a layered plate composed of two solids with perfect contact, slip, or a fluid layer at their interface, Acustica 16 (1965) 224–232.
[26] I. Viktorov, Rayleigh and Lamb Waves, Plenum, New York, 1967.

Biographies

Lianqun Zhou received his BS degree from the University of Science and Technology of China in 2003. He prepared his PhD dissertation jointly in Institute FEMTO-ST, CNRS and Changchun Institute of Optics, Fine Mechanics and Physics, Chinese Academy of Science. In 2010, he obtained his PhD from the University of Franche-Comté and the Graduate University of Chinese Academy of Sciences. Since from 2011, he became assistant professor at Suzhou Institute of Biomedical Engineering and Technology, Chinese Academy of Sciences. His research mainly involves studying the membrane–fluid interaction with micro Lamb wave sensor.

Jean-François Manceau was graduate student in electrical engineering at the Ecole Normale supérieure de Cachan (France) and received the Agregation degree in 1991, DEA (Master) degree in 1992 and joined the LPMO in Besançon, France (now included in FEMTO-ST Institute) to work on ultrasonic microactuators. In 1996, he received a PhD from the University of Franche-comté and had been Assistant Professor until 2004. He is currently Professor at the University of Franche-Comté at the Micro Nano Sciences and Systems (MN2S) Department of FEMTO-ST Institute. His current researches include acoustic interactions with fluids for sensors mainly based on Lamb waves. Actuation applications and micro-actuators for microfluidic applications, such as acoustic droplets mixing and manipulation, are also part of his current research interests.

François Bastien was born in 1941, is professor emeritus at University of Franche-Comté (Besançon, France). During 45 years he works in many fields including plasma physics, gas discharges, piezoelectricity, acoustics, sensors, actuators and microsystems. His current research included Lamb waves sensors. He is co-author of about 100 papers in journals or conference proceedings.